J. Biochem. 125, 460-468 (1999)

An Intrinsic DNA Curvature Found in the Cyanobacterium *Microcystis aeruginosa* K-81 Affects the Promoter Activity of *rpoD1* Encoding a Principal Sigma Factor[1]

Munehiko Asayama,* Youji Hayasaka,* Mamiko Kabasawa,* Makoto Shirai,*,[2] and Takashi Ohyama†

*Laboratory of Molecular Microbiology, School of Agriculture, Ibaraki University, Ami 3-21-1, Inashiki-gun, Ibaraki 300-0332; and †Department of Biology, Faculty of Science, Konan University, Okamoto 8-9-1, Higashinada-ku, Kobe 658-0072

Received September 14, 1998; accepted November 18, 1998

The *rpoD1* gene in the unicellular cyanobacterium *Microcystis aeruginosa* K-81 encodes a principal sigma factor of RNA polymerase and is transcribed under light and dark conditions to produce multiple monocistronic transcripts. In the 5′-upstream region from *rpoD1* Promoter 2, which has a sequence of *Escherichia coli* type, we found a sequence-directed DNA curvature with an AT-rich sequence. Insertions of 2 to 21 base pairs introduced into the curved center changed a gross geometry of the original curved DNA structure. The *rpoD1* promoter activities assayed *in vivo* by using transcriptional *lacZ* fusions were correlated with the change in the gross geometry in not only a cyanobacterium but also *E. coli*. In addition, RNA polymerase binding to the *rpoD1* promoter region and the efficiency of the mRNA synthesis from the *rpoD1* Promoter 2 were also affected *in vitro* by the change in the geometry. These results suggest that the tertiary structure of the curved DNA is important for the *rpoD1* transcription. The deletion of the center region of the curvature resulted in a considerable reduction of the transcription from Promoter 2 in the cyanobacterium. This report demonstrates that a curved DNA plays a significant role in transcription in cyanobacteria, and that this functional curvature is located in the 5′-upstream region from the *rpoD* gene, which encodes a principal sigma factor in eubacteria.

Key words: cyanobacteria, bent DNA, RNA polymerase, *rpoD*, transcription.

It is generally accepted that the ancestors of cyanobacteria gave rise to plant plastids by endosymbiotic events, thereby conferring the ability for photosynthesis to algae and plants. Members of the genus *Microcystis* (*Synechocystis*) are cyanobacteria (blue-green algae) which perform oxygenic photosynthesis involving two photosystems, PS I and PS II, as do higher plants. One such member, the unicellular colony-forming *Microcystis aeruginosa* strain K-81 (hereafter referred to as K-81) was isolated (*1*), and its biological features, *e.g.*, restriction-modification systems and toxins, were characterized (*2-4*). K-81 also contains the *psbA2* gene, which encodes a D1 homolog as a core protein in PS II, and which exhibits light-dependent and rhythmic expression (*5*). Although the light-dependent and circadian-rhythmic gene expression are unique properties of cyanobacteria, the transcriptional regulation of the gene expression is not fully understood. An RNA polymerase holoenzyme containing a sigma factor plays a central role in the transcription of eubacterial genes (*6*). Primary sigma factors are known to be indispensable for the maintenance of basal gene expression in vegetative cells, while alternative sigmas recognized subsets of promoter sequences. Cyanobacteria generally possess several kinds of an *rpoD* homolog (*Escherichia coli rpoD* type), and the *rpoD1* gene which encodes a principal sigma factor was isolated from the K-81 strain (*7, 8*). The monocistronic *rpoD1* transcripts from the transcriptional start points, P1 and P2, and the corresponding gene product (σ^{A1}) constitutively appeared in the K-81 cells, irrespective of light or dark conditions (*7*). The *rpoD1* 5′-upstream region containing two promoters (Promoters 1 and 2) consists of AT-rich and highly repetitive GC-rich (REP-B) sequences (*7, 9, 10*). The effects of the *cis*-elements on the *rpoD1* promoter activities have not yet been determined in the phototrophic bacterium.

It is known that the tertiary structure of DNA affects gene expression, and sequence-directed (intrinsic, static) or protein-induced DNA bends refer to changes in the DNA double helix conformations. In the former, regular runs of

[1] This work was supported by a grant for Scientific Research on Priority Areas from the Ministry of Education, Science, Sports, and Culture of Japan.

[2] To whom correspondence should be addressed. Tel: +81 298 88 8652, Fax: +81 298 88 8653, E-mail: shirai@agr.ibaraki.ac.jp

Abbreviations: bp, base pair(s); $E\sigma^{70}$, *E. coli* homologous RNA polymerase holoenzyme containing σ^{70}; $E\sigma^{A1}$, K-81 homologous RNA polymerase holoenzyme containing σ^{A1}; $^{*}E\sigma^{A1}$, RNA polymerase fraction containing σ^{A1} partially purified from the *M. aeruginosa* K-81 strain; $E+\sigma^{A1}$, heterologous RNA polymerase holoenzyme reconstituted with *E. coli* core enzyme and recombinant K-81 σ^{A1}; nt, nucleotide(s).

several deoxy adenine•deoxy thymine (dA•dT) base-pairs occur on one face of the DNA helix, while in the latter, a profound influence on DNA-protein interaction causes the bending (*11*). These flexures are known to be associated with replication, transcription, and recombination (*12-15*). However, curvatures and their biological importance for gene expression have not been characterized in cyanobacteria, algae, and plants, which are photosynthetic organisms. In this article, we report that an intrinsic DNA curvature exists in the region just upstream from K-81 *rpoD1* Promoter 2. The structure of the curved DNA and its effect on the transcription were investivated in cyanobacteria.

EXPERIMENTAL PROCEDURES

Bacterial Strains and Media—*E. coli* JM109 cells harboring plasmids were cultivated at 37°C in 2×TY liquid medium (*16*) containing 75 μg/ml ampicillin. Cyanobacterium *Synechococcus* sp. strain PCC 7942, of which the chromosomal DNA contains an insertion of the *rpoD1-lacZ* fusion construct, was grown at 30°C in BG11 liquid medium or plate (*17*) containing 20 μg/ml spectinomycin under continuous white-light illumination (1,900 lux).

Oligonucleotides—The synthetic oligonucleotides used were as follows: *Xho*I-2F (5′-CGTGTCGCTAAAATCCC-A*CTCGAG*CACAAGAGAATTTAAGCAAAAATC, 48-mer, italic: an *Xho*I site); 10F (TCGAGTCA, 8-mer); 10R (TCGATGAC, 8-mer); 15F (TCGAGTCAGTCAG, 13-mer); 15R (TCGACTGACTGAC, 13-mer); 21F (TCGAGTCAGTCAGCAGTC, 19-mer); 21R (TCGAGACTGACTGACTGAC, 19-mer); PCR-F (*GAATTCGGATCC*GATCGGATTTAAGTCCTCCAGCCATTTACCC, 43-mer, italic: *Eco*RI or *Bam*HI site); Primer 1, AAGGGTTAGTACATCGTGGG, 20-mer (*7*).

Plasmid and Phage Construction—For deletion construction, the plasmid pKXC-R [pUC119+a 1.8 kb *Xba*I fragment (positions 1 to 1768, partially shown in Fig. 1D) carrying the *rpoD1* upstream region] was digested with *Kpn*I and *Eco*RV, and the resultant fragment was deleted by exonuclease III (*18*) and self-ligated to create pKXCR-Δ103, which contains only the 5′-upstream region (positions 1 to 793) of *rpoD1* (DDBJ accession No. D85684). The plasmid pKXC3 (*7*), which contains an opposite-direction version of the insert used for pKXC-R, was digested with *Kpn*I and *Bam*HI, and the resultant fragment was also deleted by exonuclease III to construct a series of pKXCΔ plasmids: pKXCΔ2077 (containing the upstream region of positions 582 to 1768), Δ2022 (positions 630 to 1768), Δ1175 (positions 690 to 1768), and Δ1022 (positions 741 to 1768). For the circular permutation analysis, the plasmid pKXCRΔ103 was digested with *Pvu*I (at position 574) and *Eco*RI (at the multiple cloning site on the vector), and the resultant 234 bp *Pvu*I-*Eco*RI fragment [a 220 bp segment (the positions 574 to 793)+a 14 bp sequence derived from the vector] was filled in with Klenow fragment. This fragment was blunt-end ligated with *Bam*HI-digested pUC119 (*19*) to yield pEPV23. To construct a tandem dimer of the 234 bp *Pvu*I-*Eco*RI fragment, two segments of *Hin*dIII-*Sma*I and *Acc*I blunt-ended with Klenow fragment-*Eco*RI were isolated from pEPV23 and introduced into a *Eco*RI-*Hin*dIII site of pUC119 to create pCPM1 (Fig. 1A). This ligation generated a new *Sau*3AI site (Fig. 1A) located adjacent to the *Pvu*I site at the junction region on the plasmid. For insertional mutants of the curved DNA, an *Eco*RI (at the multiple cloning site)-*Eco*RV (at position 925) fragment which carries the deleted *rpoD1* 5′-upstream region was isolated from pKXCΔ2077 and inserted into the *Eco*RI-*Sma*I site of pUC119B, which contains a unique *Bgl*II site between the *Pst*I and *Sph*I sites of pUC119, to yield pKXCΔ2077B containing the region from the positions 582 to 925. An *Eco*RI-*Hin*dIII small fragment was isolated from pKXCΔ2077B and inserted into the *Eco*RI-*Hin*dIII site of a phage M13mp19 (*20*) to create φM13Δ2077B. Single-strand DNA from φM13Δ2077B was subjected to site-directed mutagenesis with Primer *Xho*I-2F to make φM13Δ2077B+2 (2 bp insertional mutant, +2), which possesses a new *Xho*I site adjacent to the bending center (Fig. 2). This φM13Δ2077B+2 also contains a second *Xho*I site located near the *Sac*I position in the multiple cloning site of the vector. To remove the second *Xho*I site, an *Sac*I blunt-ended with Mung Bean nuclease-*Hin*dIII fragment was isolated from φM13-Δ2077B+2, and this fragment was inserted into a *Bam*HI (treated with Mung Bean nuclease)-*Hin*dIII site of pUC-119B to yield construct pKXCΔ2077B+2, which possesses only one *Xho*I site on the vector. The plasmid pKXC-Δ2077B+0 (no insertion, wild-type) was also created by the procedure described above, using pKXCΔ2077B instead of φM13Δ2077B. A set of two oligonucleotides, 10F and 10R (15F and 15R, 21F and 21R), was incubated at 65°C for annealing (Fig. 2), and the resultant double-strand segment was phosphorylated by T4 polynucleotide kinase and inserted into the *Xho*I site (treated with alkaline phosphatase) of pKXCΔ2077B+2 to yield pKXC-Δ2077B+10 (+15 or +21), which carries an insertion of 10 (15 or 21) bp. To construct the 6 bp insertional mutant (pKXCΔ2077B+6), pKXCΔ2077B+2 was digested with *Xho*I, and the resultant fragments were filled in and self-ligated. The nucleotide sequence of each construct on the pKXCΔ2077B+0, +2, +6, +10, +15, and +21 plasmids was verified according to the dideoxy procedure (*21*). For *rpoD1-lacZ* fusions, pKXCΔ2077B+0, +2, +6, +10, +15, and +21 plasmids were digested with *Sma*I and *Bgl*II, and the relevant *Sma*I and *Bgl*II fragment carrying the *rpoD1* Promoters 2 and 1 was inserted into the *Sma*I-*Bgl*II site of pAM990 (*22*) to create pD1Δ2077B+0, +2, +6, +10, +15, and +21, respectively. Small *Eco*RI-*Eco*RV fragments which contain the 5′-upstream region of *rpoD1* were also isolated from pKXCΔ2022, Δ1175, and Δ1022, then inserted into the *Eco*RI-*Sma*I site of pUC-119B to yield pKXCΔ2022B, Δ1175B, and Δ1022B, respectively. Small *Eco*RI (blunt-end by Klenow)-*Bgl*II fragments were also isolated from these constructs, and inserted into the *Sma*I-*Bgl*II site of pAM990 to create pD1Δ2022B, Δ1175B, and Δ1022B, respectively.

Site-Directed Mutagenesis—Site-directed mutagenesis with Primer *Xho*I-2F and a single-stranded DNA derived from φM13Δ2077B was carried out as described previously (*23*).

Circular Permutation Analysis—The center-site of a static bend of DNA was determined by circular permutation analysis (CPA) (*10*). Permuted fragments were subjected to electrophoresis (20 mA, current constant) with a 5% polyacrylamide gel with TBE buffer (*24*) at various temperatures.

Transformation and Hybridization—To examine the effects of the curved DNA structure on the gene expression, the pD1⊿ series of plasmids were introduced into *Synechococcus* sp. strain PCC 7942 (now called PCC 7942) cells by natural transformation (*17*), then the transcriptional *lacZ*-reporter genes were inserted into a neutral site on the chromosomal DNA by homologous recombination. Recombinations were confirmed by genomic Southern hybridization using an *Eco*RI-*Hin*dIII fragment from pKXC⊿2077B as a K-81 *rpoD1*-specific probe. The host *E. coli* JM109 cells were also transformed with these pD1⊿ plasmids, which possess an *E. coli* origin (*17, 25*).

β-Galactosidase Assay—For the assay in *E. coli*, recombinant JM109 harboring *lacZ*-fusion constructs was cultured in 5 ml of 2×TY liquid medium containing 75 μg/ml ampicillin and 20 μg/ml spectinomycin at 37°C until the optical density at 600 nm reached 0.6 to 0.8 in the log-phase of growth. Portions of 0.65 ml of cultures were centrifuged in a microtube, and the pellets were stored at −80°C until use. β-Galactosidase activities for the transcriptional *rpoD1* expression were measured as described by Miller (*26*) with modifications as follows: the cell pellets were suspended in 0.6 ml of Z buffer [60 mM $Na_2HPO_4 \cdot 12H_2O$, 40 mM $NaH_2PO_4 \cdot 2H_2O$, 10 mM KCl, 1 mM $MgSO_4 \cdot 7H_2O$, 50 mM β-mercaptoethanol], and 6 μl of 10% (v/v) Triton X-100 (Sigma, St. Louis, MO) was added to the suspension. These samples were then vigorously vortexed by use of a micro-mixer (EM-33, TAITEC, Tokyo) at speed level 3 for 10 s. Orthonitrophenylgalactoside (ONPG; 4 mg/ml in 0.2 ml of 0.1 M sodium phosphate buffer, pH 7) was immediately added, and the samples were incubated at 28°C for 5 to 100 min until sufficient yellow color developed. The reaction was stopped by adding 0.3 ml of 1 M Na_2CO_3 with stirring. The cells were removed by centrifugation for 5 min, and the absorbance of the supernatant was measured at 420 nm. The β-galactosidase activity was expressed according to the following equation: β-galactosidase unit = $1{,}000 \times A_{420} \times t\ (\text{min})^{-1} \times V\ (\text{ml})^{-1} \times A_{600}{}^{-1}$ (for *E. coli*, or $A_{750}{}^{-1}$ for PCC7942). In the equation, t represents the time of the enzymatic reaction in min, V is the volume of the culture used in the assay in ml, and $A_{600}{}^{-1}$ (or $A_{750}{}^{-1}$, see below) reflects the cell density just before the assay. In the assay of recombinant PCC 7942, the cells were cultivated at 30°C in the BG11 liquid medium for 7 days (log-phase of cell growth) under continuous white-light illumination, then 1 ml of the cell culture was withdrawn, and the cell density was measured at 750 nm ($0.7 < A_{750} < 1$). The cell pellets were collected by centrifugation, and the β-galactosidase assay was conducted as described above except as follows: the cell pellets were suspended in 1 ml of Suspension buffer [10 mM Tricine (Sigma), 5 mM ε-amino-*n*-caproic acid (Wako, Osaka), 1 mM benzamide (Wako)], 10 μl of 100 mM phenylmethylfluorosulfate (PMSF, Sigma)], and 50 μl of 10% triton X-100 was added to a 0.5 ml portion of the suspension. The sample was vortexed for 10 s, then incubated at 28°C for 15 min prior to the addition of 0.2 ml of the ONPG solution. All β-galactosidase values presented in this study are the means of triplicate experiments.

Gel-Shift Assay—The binding of protein to the fragment was carried out in 15 μl of the reaction mixture [50 mM Tris-HCl (pH 8.0), 50 mM KCl, 0.5 mM EDTA-2Na (pH 8.0), 10% (v/v) glycerol, 2 mM DTT, 30 mM KCl, 3 mM $MgCl_2$, 0.1 mM ATP, 0.0001% (w/v) salmon sperm DNA (0.01 μg), and 0.0001% (w/v) bovine serum albumin (0.01 μg)] containing 0.36 pmol (0.4 μl) of *E. coli* $E\sigma^{70}$ (or a heterologous RNA polymerase reconstituted with *E. coli* core enzyme and K-81 σ^{A1}) and 0.6 pmol (2 μl) of ^{32}P-end-labeled PCR fragments amplified with template DNAs of pKXC⊿2077B+*n* (see "*Plasmid and Phage Construction*") and primers of PCR-F and Primer 1, respectively. After incubation for 7 min at 30°C, 2 μl of sample buffer consisting of 50% (v/v) glycerol, 0.1% (w/v) xylene cyanol FF, and 0.1% (w/v) bromophenol blue was added, and the resulting mixture was immediately loaded onto a 6% (w/v) polyacrylamide slab gel containing 8 M urea. After electrophoresis at a constant current (70 mA) with TES buffer containing 40 mM Tris-HCl (pH 7.9), 1 mM EDTA-2Na (pH 8.0), and 5 mM sodium acetate, the gel was subjected to autoradiography with an X-ray film (RX: Fuji, Tokyo). The signal intensity of the band due to protein-DNA complex was measured by use of Ultraviolet BIO-PROFIL (Vilber Lourmat, Cedex, France), and the relative RNA polymerase-binding activities were plotted.

In Vitro Transcription Assay—The effect of mutant curvature on the *rpoD1* mRNA synthesis from Promoter 2 with RNA polymerase holoenzymes, $E\sigma^{70}$ or $^*E\sigma^{A1}$ (*8*), was measured by primer extension analysis following multiple-round run-off transcription (*7, 8*) with modifications as follows. The assay mixture (40 μl) was comprised of 50 mM Tris-HCl (pH 8.0), 0.05 mM EDTA·2Na, 0.5 mM DTT, 5 mM $MgCl_2$, 0.1 mM each ATP, CTP, GTP, and UTP, 4.9 pmol (1 μg, 1 μl) template DNAs generated by the PCR (see "*Gel-Shift Assay*"), and 0.9 pmol (0.4 μg, 1 μl) of $E\sigma^{70}$ or 2 μl of $^*E\sigma^{A1}$. The mixture was incubated at 30°C for 10 min, then the reaction was stopped by addition of stop solution (140 μl) comprised of 40 mM EDTA·2Na and 300 μg/ml of *E. coli* tRNA. The RNA products were precipitated with 2-propanol and then dissolved in 10 μl of water. The 5′-end mapping of the *rpoD1* transcript from Promoter 2 was carried out in reaction mixture (20 μl) comprised of 10 μl of the mRNA solution mentioned above, 4 μl of 5×First-strand buffer (*7*), 2 μl (1 pmol) of ^{32}P-end-labeled Primer 1, 2 μl of DTT (100 mM), 1 μl of dNTP (20 mM), and 1 μl of a reverse transcriptase (200 units). The products recovered by ethanol precipitation were dissolved in 10 μl of the stop solution. After denaturation at 95°C for 3 min, 2 μl aliquots of the samples were resolved by electrophoresis on a 6% DNA sequencing gel. The signal intensity of the band due to the *rpoD1* transcript from Promoter 2 was analyzed by the procedure described above for the gel-shift assay.

RESULTS

Intrinsic Bend of DNA in the 5′-Upstream Region of rpoD1 Promoter 2—Recent studies have demonstrated the existence of sequence-directed DNA bends in AT-rich DNA sequences which contain periodical dA_n and/or dT_n tracts (usually $n \geq 3$) along the same face on the DNA helix (*10*). The upstream region, involving Promoters 1 and 2 (Fig. 1D), of the *Microcystis aeruginosa* K-81 *rpoD1* gene also consists of an AT-rich nucleotide sequence (566 bp, positions 266 to 831 from a *Xba*I site shown as "1"). We first assessed whether the *rpoD1* promoter around the region contains a detectable bent DNA structure by measuring the electrophoretic mobility of a fragment containing the

AT-rich region. First, the plasmid pKXCR⊿103 (see "EXPERIMENTAL PROCEDURES"), which contains a region consisting of a highly repetitive sequence, REP-B, that is GC-rich (G+C=59.4%, positions 1 to 265) and almost the entire AT-rich sequence (A+T=61.5%, positions 266 to 793), was digested with *Sau*3AI. Portions of 1 μg of *Sau*3AI fragments were incubated with various amounts of distamycin A, and the resultant fragments were subjected to polyacrylamide gel electrophoresis (PAGE) at a low temperature, 13°C. In the absence of distamycin A, a *Sau*3AI fragment of approximately 350 bp containing the *rpoD1* 5′-upstream region (positions 570 to 793, Fig. 1D) plus an additional sequence of about 130 bp from the vector exhibited anomalously low mobility. It behaved as if it had been an about 430 bp fragment on the original gel (data not shown). It is known that distamycin A binds to the AT-rich minor groove on the DNA helix and is able to diminish DNA compression, resulting in anomalous migration of such curved DNA fragments on the gel (*11*). The addition of distamysin A gradually diminished the anomalous migration (data not shown), suggesting that the *rpoD1* 5′-upstream region contains an intrinsic DNA curvature.

We therefore carried out circular permutation analysis in order to determine the center region of the curved DNA. A *Hin*dIII-*Eco*RI fragment carrying the tandem dimer to be analyzed was isolated from pCPM1 and digested with restriction enzymes whose sites occur once in each unit of the dimer (Fig. 1A). These permuted fragments (filled bars in Fig. 1A) exhibited different migrations on PAGE at 10°C (Fig. 1B). The mobilities of the permuted fragments are plotted against the position of the restriction site in one unit of the tandem dimer (Fig. 1C). The graph indicates that the bent center is located upstream of *rpoD1* Promoter 2 (immediately upstream of the *Mbo*II site in Fig. 1D). This locus is depicted on a cylindrical projection of the DNA with 10.5 bp per turn (Fig. 1D, filled circles). Several dA•dT and dT•dA tracts are periodically located on the same face of the DNA helix in this region, 574 to 793. The previous study developed an empirical relationship between the mobility of the fragments in circular permutation analysis and the bending angle (*27*). This is expressed by the equation $\mu M/\mu E = \text{cosine } \alpha/2$, where μM is the mobility of the fragment with the bent sequence closest to the middle (slowest; in this case, the *Xba*I fragment), and μE is the mobility of the fragment which contains the bent sequence

```
+0  AGCATTCCGTGTCGCTAAAATCCCATCGACACAAGAGAATTTAAG
+2  CATTCCGTGTCGCTAAAATCCCA[redacted]CACAAGAGAATTTAAG
+6  CCGTGTCGCTAAAATCCCACTCGATCGAGCACAAGAGAATTTAAG
+10 GTCGCTAAAATCCCACTCGAGTCATCGAGCACAAGAGAATTTAAG
+15 TAAAATCCCACTCGAGTCAGTCAGTCGAGCACAAGAGAATTTAAG
+21 CCCACTCGAGTCAGTCAGTCAGTCTCGAGCACAAGAGAATTTAAG
```

Fig. 2. **Nucleotide sequences of the mutant-promoter constructs.** The 5′-upstream region from *rpoD1* Promoter 2 shown is the same as in Fig. 1D. The oligonucleotide insertions for each mutant are underlined, and the runs of adenine or thymine are in bold types. A created *Xho*I site on the +2 mutant is represented by a shaded box.

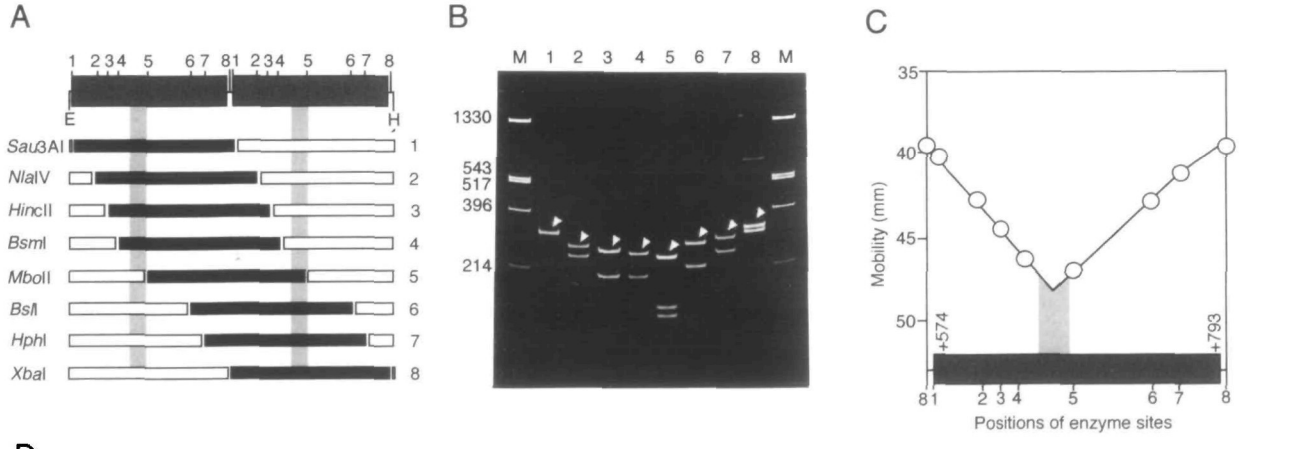

Fig. 1. **Circular permutation analysis.** (A) Structure of a tandem dimer (gray bold bars) of the 220 bp fragment containing the *rpoD1* 5′-upstream region (+574 to +793, Fig. 1C) and the 234 bp permuted segments (each filled bar) used for the analysis. The *Eco*RI (E)-*Hin*dIII (H) fragment of approximately 480 bp carrying the dimer was isolated from pCPM1 ("EXPERIMENTAL PROCEDURES"), and digested with each restriction enzyme. The numbers 1 to 8 indicate restriction sites on the dimer. The vertical gray bars show the curved center revealed by the plot shown in Fig. 1C. (B) 5% PAGE at 10°C. The *Eco*RI-*Hin*dIII fragments (Fig. 1A) digested with each enzyme were subjected to PAGE. Lanes are indicated according to the fragment numbers. The bands of interest are indicated with white arrowheads. A molecular size marker (plasmid pUC119 DNA digested with *Hin*fI) is shown in lane M (size in base pairs). (C) Mobility plot of the permuted fragments. The mobilities of permuted fragments on the gel (Fig. 1B) are plotted against the position of the restriction site in one unit of the tandem dimer shown in Fig. 1A. (D) The nucleotide sequence of the 5′-upstream region of *rpoD1* is shown with nucleotide numbers from the *Xba*I site as +1. The positions of the restriction enzyme sites, Promoter 2, and its transcriptional start point P2 are also shown. The sequence which surrounds the curved center (arrowheads) is depicted on a cylindrical projection with 10.5 bp (filled circles) per one pitch for the DNA helix, and the stretches of dA_n or dT_n tracts ($n \geq 3$) in the upstream region are marked by shaded boxes. The 5′-ends of the insert *rpoD1* fragment on each deletion plasmid (Fig. 7) are shown.

near the end (fastest; in this case, the *Mbo*II fragment). When this equation is applied, it predicts that this permutated fragment has a bending angle of about 60 degrees at 10°C.

Alteration of the Curved DNA Structure by Insertional Mutations at the Bending Center—To characterize the stimulation of the *rpoD1* transcription by the intrinsic DNA curvature, a series of mutant promoters with various synthetic oligonucleotides (+2, 6, 10, 15, and 21 bp) inserted at the center region of curvature was constructed (Fig. 2). These insertions slightly increased the distance between the upstream and downstream halves of the curved DNA, and they also rotated the upstream half around the helical axis with respect to the downstream half containing the −35 and −10 regions of *rpoD1* Promoter 2. The 2, 6, 10, 15, and 21 bp inserts generate rotational displacements of 69, 206, 343, 154, and 360 degrees, respectively (Fig. 2). To test for the altered DNA conformations, each of the pKXCΔ2077B+0, +2, +6, +10, +15, and +21 plasmid DNAs was digested with *Eco*RI (this site exists in the multiple cloning site of each vector) and *Tfi*I (the position of 791), and the resultant 220-241 bp *Eco*RI-*Tfi*I fragments containing such inserts at the center of the curvature were subjected to PAGE at 4, 30, and 45°C (Fig. 3). It has been reported that the electrophoretic mobility of the intrinsic curvature returns to normal at higher temperatures (*24, 28-30*). The fragments carrying the inserts of dinucleotides (+2) and hexanucleotides (+6), despite being longer than the wild-type fragment (+0), moved faster than the wild-type fragment at 30°C (Fig. 3A). The fragment carrying a +15 insert showed higher electrophoretic mobility than the fragment carrying a +10 insert. The ratio of expected (Ex)/actual (Ac) mobilities (=relative mobility, RM) did not remain constant, and reached a maximum for the +10 or +21 insert fragments, and a minimum for the +6 or +15 fragments at each temperature (Fig. 3B). By reference to the theoretical study (*31*), our results are explained as follows. The runs of A or T in the region from 640.5 (the center of the A4 tract) to 718 (Fig. 1D) lie at a mean helical repeat of 11.1 bp (718−640.5=77.5 bp, 77.5/7=11.1), *versus* a twist repeat in the DNA of 10.5 bp. The region thus presumably forms a small part of a right-handed coil. The inserts made new curvature repeats of (77.5+2)/7=11.4, (77.5+6)/7=11.9, (77.5+10)/8=10.9, (77.5+15)/8=11.6, and (77.5+21)/9=10.9 bp, respectively. The 2, 6, and 15 bp inserts moved faster in the gel, since the fragments containing these inserts became more superhelical (with mean helical repeats of 11.4, 11.9, and 11.6, respectively). The 10 and 21 bp inserts moved at similar rates to the wild-type, since these inserts largely retained the planarity of the original curvature. Thus, the mean helical repeats of the curvatures of pKXCΔ2077B+0, +10, and +21 are similar to each other, as are those of pKXCΔ2077B+6, and +15. The similarities in the RM values for these fragments at 30°C in Fig. 3 [RM=1.13 (pKXCΔ2077B+0), 1.11 (+10), and 1.12 (+21), 1.04 (+6) and 1.06 (+15)] seem to support this idea experimentally. These results also reinforce the notion that the gross geometry of the curved DNA was periodically altered by the inserts, and the cyclical pattern shown in Fig. 3B implies that the conformations of the curvatures carrying the +6 and +15 inserts are completely different from those carrying the +10 and +21 inserts (as well as +0; wild type). However, judging from the RM values, the intrinsic curved structures seemed to still exist even at the high temperature of 45°C (Fig. 3B).

Effects of the Insertions on In Vivo and In Vitro Activities of the rpoD1 Promoter—Various inserts alter the gross geometry of the DNA curvature located in the region upstream from Promoter 2. We next wished to learn how this alteration affects *rpoD1* transcription *in vivo* and *in vitro*. Since the K-81 strain has a strong restriction barrier composed of an extracellular nuclease and restriction endonucleases (*3, 4*), no transformation system has been established, and biological analyses of the mutant curvatures are accordingly difficult. However, a Promoter 2-dependent specific *rpoD1* transcript has been observed in a unicellular cyanobacterium, PCC 7942 (Fig. 4), and analyses in these heterologous cells may provide essential clues for understanding the role of K-81 *rpoD1* transcription.

First, the mutant *rpoD1* promoter activities on the *lacZ*-fusion constructs were measured in the recombinant PCC 7942 cells. To avoid the titration effect by gene dosage that is sometimes observed in bacteria for gene expression *in trans* when a target gene on a multicopy vector is

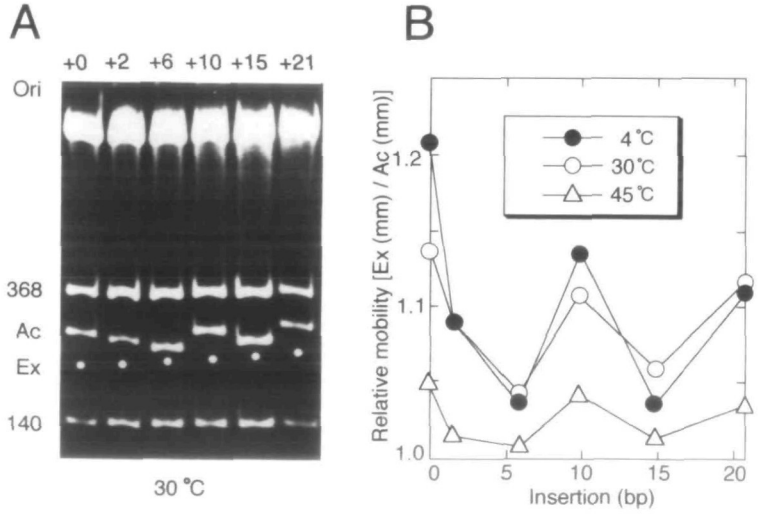

Fig. 3. **Alteration of the gross geometry of the curved DNA by insertions.** (A) One microgram of each plasmid pKXCΔ2077B+*n* (*n*=0, 2, 6, 10, 15, and 21), which contains the insertion at the curved center, was digested with *Eco*RI and *Tfi*I (see "RESULTS"), and then the resultant fragments were subjected to 6% PAGE at 30°C. The positions of the 368 and 140 bp fragments which do not carry the curved DNA are shown at the left. The positions of expected (Ex, white circles) and actual (Ac) mobilities of the fragments containing the curved DNA are also shown. The gel origin (Ori) is also represented. (B) Relative mobility (RM), expressed as the ratio of expected to actual electrophoretic mobility (mm), was calculated from PAGE gels run at 4, 30, and 45°C.

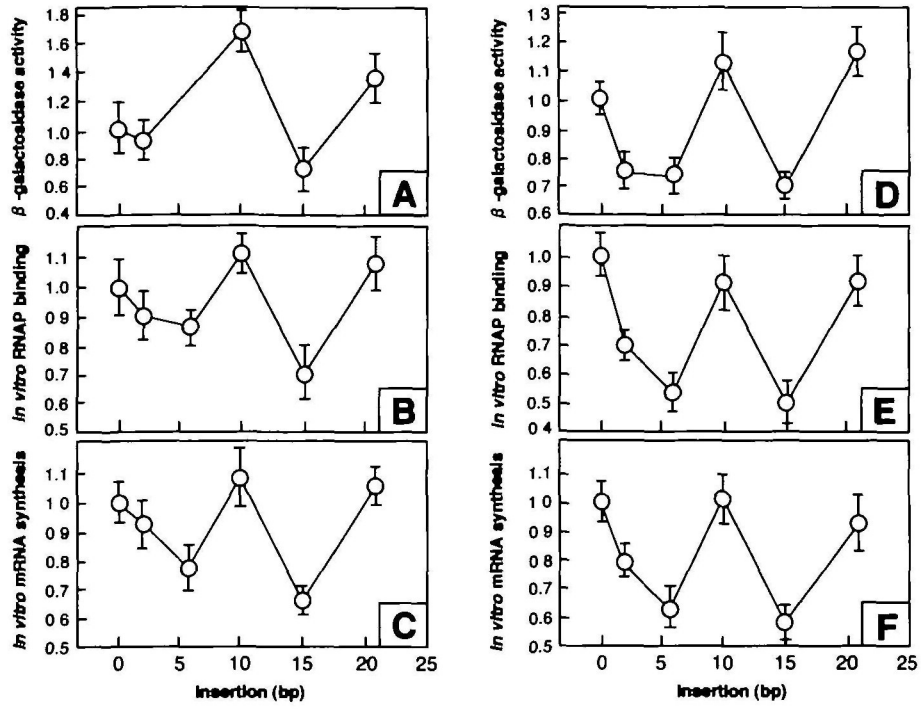

Fig. 4. **Effect of insertional mutations on the *rpoD1* transcription.** [β-Galactosidase activities] The *rpoD1* promoter-dependent activities were measured in the PCC 7942 (A) or *E. coli* JM109 (D) cells transformed with plasmids (pD1⊿2077B+*n*: *n*=0, 2, 6, 10, 15, and 21). The results are expressed in Miller units. [Binding activities] Relative RNA polymerase (RNAP) holoenzyme binding activities of *E. coli* core+K-81 σ^{A1} (B) or *E. coli* Eσ^{70} (E) against the constant mol of the fragment were plotted. The fragments (307, 309, 313, 317, 322, and 328 bp containing +0, +2, +6, +10, +15, and +21 insertions, respectively) were amplified by PCR with primers of PCR-F and Primer 1, then ^{32}P-end-labeled. Portions of 0.6 pmol of these fragments were subjected to gel-shift assay with 0.36 pmol of RNAP. [mRNA synthesis] The *rpoD1* transcripts synthesized from Promoter 2 with mutant curvatures were analyzed by primer extension analyses following multiple-round run-off transcription with the PCR fragments shown in the binding assay and K-81 *Eσ^{A1} (C) or *E. coli* Eσ^{70} (F). All relative values in the six panels were averaged from three separate experiments and then normalized. Error was less than 15%.

introduced into the host cell, and to better understand the role of the curved DNA in the genome of cyanobacterium, the *lacZ*-fusion constructs on pD1⊿2077B+*n* were inserted into the neutral site of the PCC7942 chromosome by homologous recombination, and then β-galactosidase activities were measured (Fig. 4A). The results showed that the most efficient mutant promoters contained 10 and 21 bp insertions, and the insertion of 15 bp resulted in the least efficient mutant promoters in PCC 7942. This result was compatible with that in Fig. 3B, indicating that three-dimensional architecture of the curved DNA correlates with the promoter activities. Interestingly, the insertions of 10 and 21 bp slightly increased the *in vivo* promoter activity. In this experiment, we were unable to construct a mutant harboring the +6 insert. Unfavorable modifications of the original curvature might not be tolerated by the cell. Next, to asertain whether the differences in *in vivo* promoter function reflect the differences in the affinity of RNA polymerase for various insert mutants, the binding affinity of a heterologous RNA polymerase holoenzyme (E+σ^{A1}) reconstituted using *E. coli* core enzyme and K-81 σ^{A1} (the *rpoD1* gene product) to the wild-type and mutant promoters was examined. The result presented in Fig. 5 was generated at an RNA polymerase/DNA molar ratio of 0.6 ("EXPERIMENTAL PROCEDURES") and at 30°C, where curved DNA conformations still existed (Fig. 3). When no protein of the RNA polymerase was added (Fig. 5, left), major signals of free DNA form 1 were observed together with unexpected minor signals of DNA form 2, which might be caused by unusual modes of curvature. The signals were shifted to a new position (complex form) by the addition of the RNA polymerases (Fig. 5, right). Since end-labeling efficiency might be slightly different for each DNA sample, the signal intensities in the absence of the RNA polymerase were not homogeneous among samples (Fig. 5, left).

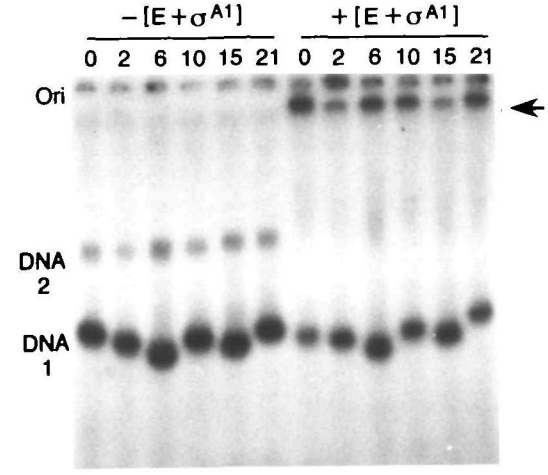

Fig. 5. ***In vitro* RNA polymerase binding.** The end-labeled PCR fragments containing the region of the *rpoD1* promoters and the mutant curvatures with insertions ("EXPERIMENTAL PROCEDURES") were subjected to gel-shift assay at 30°C with or without the heterologous RNA polymerases (E+σ^{A1}) reconstituted by an *E. coli* core enzyme (E) and a principal sigma factor of the K-81 strain (σ^{A1}). The positions of gel origins (Ori), free DNAs (DNA 1, 2) and the DNA-protein complex (arrow) are shown. The numbers at the top represent the length (bp) of inserts on each pKXC2077B+*n*.

Therefore, the binding activities were calculated as a signal intensity, according to the shifted bands with the RNA polymerases (Fig. 5, right), divided by the total signal intensity without the RNA polymerases (Fig. 5, left), and were expressed as a ratio (Fig. 4B). The binding data agreed well with results obtained from *in vivo* expression assays, also strongly indicating that the three-dimensional architecture of the curvature affects the efficiency of RNA

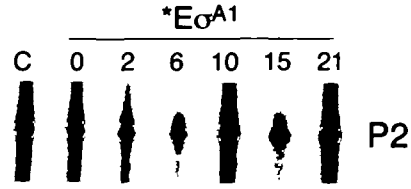

Fig. 6. ***In vitro* mRNA synthesis.** Multiple round run-off transcription assay was performed at 30°C with the PCR fragments containing the mutant curvature (Fig. 5) as template DNA and K-81 RNA polymerase fraction, *Eσ^{A1}. The 5′-end mapping of the transcripts synthesized *in vitro* was carried out by primer extension ("EXPERIMENTAL PROCEDURES"). The transcriptional start point (P2) from Promoter 2 is shown. The 5′-end of the *rpoD1* transcript in the K-81 cells grown under the 6-h light condition was determined (7) and is also indicated as a control (C).

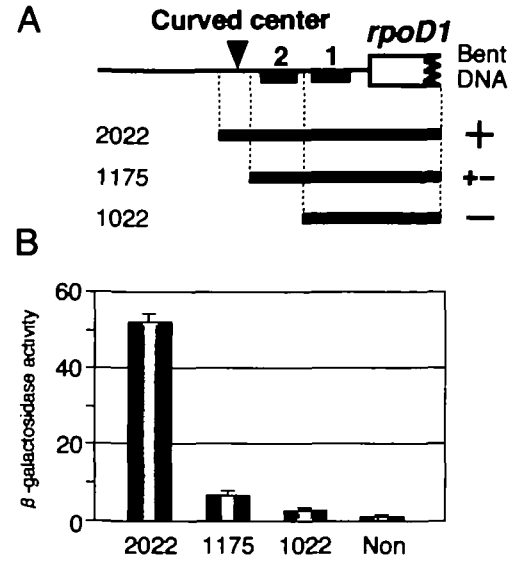

Fig. 7. **Influence of the region containing the curved DNA for the *rpoD1* transcription from Promoter 2.** (A) Transcriptional *lacZ*-fusion constructs for the K-81 *rpoD1* deletion mutants on the cyanobacterium *Synechococcus* sp. strain PCC 7942 genome are shown. (B) The relative β-galactosidase activities dependent on the *rpoD1* transcription were measured in the recombinant PCC 7942 (shown as Non; no insert), PCC7942⊿2022B, ⊿1175B, and ⊿1022B cells, respectively. Relative values are the means of triplicate experiments with the standard deviations indicated.

polymerase binding to the promoter region. Furthermore, this *in vitro* binding result encouraged us to continue investigations into the *in vitro* mRNA synthesis by K-81 *Eσ^{A1} (an RNA polymerase fraction partially purified from the K-81 cell) from *rpoD1* Promoter 2 on each linearized template, under the same conditions as those used in the binding experiments (Fig. 5, "EXPERIMENTAL PROCEDURES"). Again, it was apparent that the level of *in vitro* transcription of +10 and +21 insertions (corresponding to about 0.95 and 2.00 helical turns) was higher than those of +6 and +15 insertions (about 0.57 and 1.43 helical turns), showing that the *rpoD1* Promoter 2 activities are dependent on the gross geometry of the curvature (Figs. 4C and 6).

The *rpoD1* transcription from Promoter 2, which has an *E. coli* type sequence, by the RNA polymerase containing a principal sigma factor, K-81 σ^{A1}, was affected by the gross geometry of the curvature (Fig. 4, B and C). The amino acid sequence of σ^{A1} (the *rpoD1* gene product) exhibits extensive similarity to that of *E. coli* σ^{70} (8). Therefore, we also examined the K-81 *rpoD1* transcription from Promoter 2 with the mutant curvatures in *E. coli*. The transcriptional *lacZ*-fusion constructs (pD1⊿2077B+*n*) were introduced into the host *E. coli* JM109 cells (*recA*$^-$) in multiple copies (15–20 copies), and β-galactosidase activities in the recombinant cells were measured. The results are shown in Fig. 4D. We obtained essentially the same results using mutant curvatures with inserts as shown in Fig. 4A. It was verified that the plasmid copy numbers of these constructs in the *E. coli* cells were almost the same. In addition, it was found that *E. coli* Eσ^{70} also acted at 30°C in a similar fashion to the *in vitro* results shown in Fig. 4B (Fig. 4E). Furthermore, the *rpoD1 in vitro* transcription from Promoter 2 was also dependent on the gross geometry of the curvature in the case of *E. coli* Eσ^{70} (Fig. 4F). These results imply *in vivo* and *in vitro* functional significances of the curvature for the K-81 *rpoD1* transcription in not only cyanobacterium but also *E. coli*, suggesting a common mechanism for the transcription by RNA polymerase containing the principal sigma factors in both bacteria.

Influence on Transcription of Deletions in the Region Containing the Curved DNA—To ascertain effects of the upstream *cis*-element containing the curved center, *in vivo* analysis of *rpoD1* transcription in the cyanobacterial cells was performed as follows. The plasmids of the transcriptional *lacZ*-fusion constructs pD1⊿2022B, ⊿1175B, and ⊿1022B, and pAM990 (no-insert) were constructed (Fig. 1D) and introduced into a neutral locus on the genome of PCC 7942 as a monocopy by the same procedure described in Fig. 4A, then the β-galactosidase activities in those cells, which were named PCC7942⊿2022B, ⊿1175B, ⊿1022B, and Non (no-insert), were measured (Fig. 7). The promoter activity was recognized in the cells of PCC7942⊿2022B (carrying *rpoD1* curved center+Promoter 2+Promoter 1), whereas this value was strikingly decreased in the ⊿1175B (Promoter 2+Promoter 1) cells. In contrast, low promoter activity was apparent in the ⊿1022B (only Promoter 1) cells. The 1175 construct still possessed a feature of curved DNA, *i.e.*, anomalously low mobility on gel electrophoresis at low temperature, but it was markedly less than that of 2022, indicating that the 1175 construct has a defective curvature, whereas the 1022 construct possesses no intrinsic curvature. These results suggest that the region containing the curved center is important for the *rpoD1* transcription from Promoter 2 in the cyanobacterium. However, the biological significance of the curvature with around the sequence in the upstream region remains unresolved.

DISCUSSION

To our knowledge this is the first time that (i) an intrinsic DNA curvature was found in the upstream region from a principal sigma factor gene, and (ii) mutant curvatures were characterized with regard to their biological relevance in a photosynthetic bacterium. This curved DNA structure seems to play a significant role in the effective K-81 *rpoD1* transcription not only in the cyanobacterial cells but also in non-phototrophic *E. coli* cells. In the case of *rpoD1*, the curved DNA was found upstream of K-81 Promoter 2,

which is constitutively transcribed under both conditions of light and darkness (*7*). Therefore, this curvature can not be at least effective to light-dependent but basal (constitutive) transcription for K-81 *rpoD1*. Recently, we found that another novel intrinsic curvature, *CIT* (*30*), in the upstream promoter region from K-81 *psbA2*, of which the transcript is light-dependent under light/dark cycle conditions. Characterization of these curvatures would be important for understanding the roles of these structures in not only cyanobacteria but also higher plants.

The positions of curvature are known to vary in prokaryotic genes. These positions often exist in the region −40 to −240 from the transcriptional start point (+1), and these static DNA bends can modulate transcription (*32*). Effective *cis*-elements located far upstream (more than 300 bp) from the respective promoter can modulate the transcription associated with a *trans*-acting factor, by DNA looping (*33*). The bending center of the *rpoD1* curved DNA lies about 60 bp upstream from the Promoter 2 transcriptional start point (P2) in the AT-rich region (positions 487 to 831, A+T=57.7%) that contains Promoters 1 and 2. Although the further 5′-upstream region also contains an AT-rich sequence (positions 267 to 486, A+T=67.3%), we could not detect clear static bends of DNA in this region (data not shown). These findings also indicate that only one static bend of DNA is located in the *rpoD1* 5′-upstream region (Fig. 1), which is just 3′-downstream of a *leuA* gene (*9, 10*). In the *leuA-rpoD1* locus on the genome of K-81, the unit of multiple transcripts from the genes is monocistron each other (*7, 9*). Furthermore, AT-rich sequences can be also detected upstream of structural genes encoding principal sigma factors in other cyanobacteria. If these sequences contribute to the curved structures, basal transcription of the principal sigma factor genes may be expressed *via* the curvatures in the cyanobacteria. These possibilities are being examined in our laboratory.

Our results do not contradict those of previous studies (*34-36*). In McAllister and Achberger's report (*34*), the insertions for rotational orientation were introduced into a site between the bending center and the −35 sequence of an Alu156 promoter of *Bacillus subtilis* phage SP82. Short DNA insertions of 6-29 base pairs were used to simultaneously change the linear placement and rotational orientation, and the rotational orientation of the curved upstream DNA relative to the Alu156 promoter was of the uppermost importance for efficient promoter function. In the studies by Bracco *et al.* (*35*) and Ohyama *et al.* (*36*), segments were inserted into a site adjacent to the bending center located upstream of the gal or β-lactamase promoter in *E. coli*, respectively. The synthetic curved DNA resulted in altered gross geometry, and the promoter strength was found to be apparently dependent, in part, on the gross geometry of the curvature *in vivo*. In our study, the insertions of 6 and 15 bp seemed to alter the gross geometry of the wild-type curvature (Fig. 2) from the "U"-like shape (having a slight writhe toward the right) to the relatively "S"-like shape, and eventually caused the reduction of the *rpoD1* transcription from Promoter 2 not only *in vivo* but also *in vitro* (Fig. 4). This effect was also observed at the level of RNA polymerase binding. On the other hand, a slight increase in length of the center region of the curvature might not influence the promoter activities, as is clearly demonstrated in the results for the 10 and 21 bp inserts, suggesting that retention of the gross geometry of the DNA curvature is much more important in efficient transcription than changes in the linear placement caused by the 10 and 21 bp insertions. It has been reported that RNA polymerases cause a negative change in the linking number (*37*), and that right-handed coils are often located in regions just upstream from promoters (*38*). RNA polymerase-induced change in the sense of the superhelix from right-handed to left-handed might cause local unwinding of DNA for open-complex formation during transcription (*38*). A previous study also presented evidence *in vivo* and *in vitro* that right-handed superhelical curvatures immediately upstream of the β-lactamase promoter clearly facilitate transcription (*39*). The results obtained in this study also suggest the significance of a superhelical rightward writhe in the upstream region of a core promoter in the photosynthetic bacterium. Because the α-subunit of RNA polymerase holoenzyme may recognize the DNA configuration in the region just upstream from the promoter (*40*), the interaction between RNA polymerase and DNA writhe is of interest and should be important in transcription initiation. Further, protein-induced DNA bending by RNA polymerase also appears to be required for transcription events beyond DNA recognition, specifically for open-complex formation (*41*), raising the question of whether the *rpoD1* intrinsic curvature relates to open-complex formation in the transcription. The analyses using mutants with right- or left-handed superhelical curvatures or none, derived from an original construct (having a slight rightward writhe), may provide clues for further elucidation of the role of the three-dimensional architecture of the curved DNA for transcription. Our present observations also shed light on the importance for efficient transcription of the tertiary conformation involving the curvatures of upstream DNA in the photosynthetic organisms.

We thank Dr. S.S. Golden for providing pAM990.

REFERENCES

1. Shirai, M., Matumaru, K., Ohtake, A., Takamura, Y., Aida, T., and Nakano, M. (1989) Development of a solid medium for growth and isolation of axenic *Microcystis* strains (cyanobacteria). *Appl. Environ. Microbiol.* **55**, 2569-2571
2. Ohtake, A., Shirai, M., Aida, T., Mori, N., Harada, K., Matsuura, K., Suzuki, M., and Nakano, M. (1989) Toxicity of *Microcystis* species isolated from natural blooms and purification of the toxin. *Appl. Environ. Microbiol.* **55**, 3202-3207
3. Sakamoto, T., Shirai, M., Asayama, M., Aida, T., Sato, A., Tanaka, K., Takahashi, H., and Nakano, M. (1993) Characteristics of DNA and multiple *rpoD* homologs of *Microcystis* (*Synechocystis*) strains. *Int. J. Syst. Bacteriol.* **43**, 844-847
4. Takahashi, I., Hayano, D., Asayama, M., Futagami, M., Watahiki, M., and Shirai, M. (1996) Restriction barrier composed of an extracellular nuclease and restriction endonuclease in the unicellular cyanobacterium *Microcystis* sp. *FEMS Microbiol. Lett.* **145**, 107-111
5. Sato, M., Shibato, J., Aida, T., Asayama, M., and Shirai, M. (1996) Light-responsive and rhythmic gene expression of *psbA2* in cyanobacterium *Microcystis aeruginosa* K-81. *J. Gen. Appl. Microbiol.* **42**, 381-391
6. Lonetto, M., Gribskov, M., and Gross, C.A. (1992) The σ^{70} family: sequence conservation and evolutionary relationships. *J. Bacteriol.* **174**, 3843-3849
7. Asayama, M., Tanaka, K., Takahashi, H., Sato, A., Aida, T., and Shirai, M. (1996) Cloning, sequencing and characterization of the gene encoding a principal sigma factor homolog from the cyano-

bacterium *Microcystis aeruginosa* K-81. *Gene* **181**, 213-217
8. Asayama, M., Suzuki, H., Sato, A., Aida, T., Tanaka, K., Takahashi, H., and Shirai, M. (1996) The *rpoD1* gene product is a principal sigma factor of RNA polymerase in *Microcystis aeruginosa* K-81. *J. Biochem.* **120**, 752-758
9. Asayama, M., Kabasawa, M., and Shirai, M. (1997) A novel genetic organization: *leuA-rpoD1* locus in the cyanobacterium *Microcystis aeruginosa* K-81. *Biochim. Biophys. Acta* **1350**, 15-20
10. Asayama, M., Kabasawa, M., Takahashi, I., Aida, T., and Shirai, M. (1996) Highly repetitive sequences and characteristics of genomic DNA in unicellular cyanobacterial strains. *FEMS Microbiol. Lett.* **137**, 175-181
11. Wu, H.-M. and Crothers, D.M. (1984) The locus of sequence-directed and protein-induced DNA bending. *Nature* **308**, 509-513
12. Zahn, K. and Blattner, F.R. (1985) Sequence-induced DNA curvature at the bacteriophage λ origin of replication. *Nature* **317**, 451-453
13. Mizuno, T. (1987) Static bend of DNA helix at the activator recognition site of the *ompF* promoter in *Escherichia coli*. *Gene* **54**, 57-64
14. Ohyama, T. and Hashimoto, S. (1989) Upstream half of adenovirus type 2 enhancer adopts a curved DNA conformation. *Nucleic Acids Res.* **17**, 3845-3853
15. Yang, C.-C. and Nash, H.A. (1989) The interaction of *E. coli* IHF protein with its specific binding sites. *Cell* **57**, 869-880
16. Horowicz, D. and Burke, J.F. (1981) Rapid and efficient cosmid cloning. *Nucleic Acids Res.* **9**, 2988-2992
17. Golden, S.S. and Sherman, L.A. (1984) Optimal conditions for genetic transformation of the cyanobacterium *Anacystis nidulans* R2. *J. Bacteriol.* **158**, 36-42
18. Henikoff, S. (1984) Unidirectional digestion with exonuclease III targeted breakpoints for DNA sequencing. *Gene* **28**, 351-359
19. Vieira, J. and Messing, J. (1987) Production of single-stranded plasmid DNA. *Methods Enzymol.* **153**, 3-11
20. Sambrook, J., Fritsch, E.F., and Maniatis, T. (1989) *Molecular Cloning: A Laboratory Manual*, Cold Spring Harbor Laboratory Press, Cold Spring Harbor, NY
21. Sanger, F., Nicklen, S., and Coulson, A.R. (1977) DNA sequencing with chain-terminating inhibitors. *Proc. Natl. Acad. Sci. USA* **74**, 5463-5467
22. Golden, S.S. (1995) The Molecular Biology of Cyanobacteria: Light-responsive gene expression and the biochemistry of the photosystem II reaction center (Bryant, D.A., ed.) pp. 693-714, Kluwer Academic Publishers Press, Dordrecht
23. Kunkel, T.A. (1985) Rapid and efficient site-specific mutagenesis without phenotypic selection. *Proc. Natl. Acad. Sci. USA* **82**, 488-492
24. Asayama, M., Yamamoto, A., and Kobayashi, Y. (1995) Dimer form of phosphorylated Spo0A, a transcriptional regulator, stimulates the *spo0F* transcription at the initiation of sporulation in *Bacillus subtilis*. *J. Mol. Biol.* **250**, 11-23
25. Mandel, H. and Higa, A. (1970) Calcium-dependent bacteriophage DNA infection. *J. Mol. Biol.* **53**, 159-162
26. Miller, J.H. (1972) *Experiments in Molecular Genetics*, pp. 352-355, Cold Spring Harbor Laboratory Press, Plainview, NY
27. Thompson, J.F. and Landy, A. (1988) Empirical estimation of protein-induced DNA bending angles. *Nucleic Acids Res.* **16**, 9687-9704
28. Diekmann, S. (1987) Temperature and salt dependence of the gel migration anomaly of curved DNA fragments. *Nucleic Acids Res.* **15**, 247-265
29. Ohyama, T. (1996) Bent DNA in the human adenovirus type 2 E1A enhancer is an architectural element for transcription stimulation. *J. Biol. Chem.* **271**, 27823-27828
30. Agrawal, G.K., Asayama, M., and Shirai, M. (1997) A novel bend of DNA *CIT*: changeable bending-center sites of an intrinsic curvature under temperature conditions. *FEMS Microbiol. Lett.* **147**, 139-145
31. Calladine, C.R., Drew, H.R., and McCall, M.J. (1988) The intrinsic curvature of DNA in solution. *J. Mol. Biol.* **201**, 127-137
32. Perez-Martin, J., Rojo, F., and Lorenzo, V.D. (1994) Promoters responsive to DNA bending: a common theme in prokaryotic gene expression. *Microbiol. Rev.* **58**, 268-290
33. Matthews, K.S. (1992) DNA looping. *Microbiol. Rev.* **56**, 123-136
34. McAllister, C.F. and Achberger, E.C. (1989) Rotational orientation of upstream curved DNA affects promoter function in *Bacillus subtilis*. *J. Biol. Chem.* **264**, 10451-10456
35. Bracco, L., Kotlarz, D., Kolb, A., Diekmann, S., and Buc, H. (1989) Synthetic curved DNA sequences can act as transcriptional activators in *Escherichia coli*. *EMBO J.* **13**, 4289-4296
36. Ohyama, T., Nagumo, M., Hirota, Y., and Sakuma, S. (1992) Alteration of the curved helical structure located in the upstream region of the β-lactamase promoter of plasmid pUC19 and its effect on transcription. *Nucleic Acids Res.* **20**, 1617-1622
37. Amouyal, M. and Buc, H. (1987) Topological unwinding of strong and weak promoters by RNA polymerase: a comparison between the *lac* wild-type and the UV5 sites of *Escherichia coli*. *J. Mol. Biol.* **195**, 795-808
38. Travers, A.A. (1990) Why bend DNA? *Cell* **60**, 177-180
39. Hirota, Y. and Ohyama, T. (1995) Adjacent upstream superherical writhe influences an *Escherichia coli* promoter as measured by *in vivo* strength and *in vitro* open complex formation. *J. Mol. Biol.* **254**, 566-578
40. Ross, W., Gosink, K.K., Salomon, J., Igarashi, K., Zou, C., Ishihama, A., Severinov, K., and Gourse, R.L. (1993) A third recognition element in bacterial promoters: DNA binding by the α subunit of RNA polymerase. *Science* **262**, 1407-1413
41. Heumann, H., Ricchetti, M., and Werel, W. (1988) DNA-dependent RNA polymerase of *Escherichia coli* induces bending or an increased flexibility of DNA by specific complex formation. *EMBO J.* **13**, 4379-4381